Horticulture Research

Horticulture Research, 2022, **9**: uhab016
https://doi.org/10.1093/hr/uhab016

Article

Aluminum can activate grapevine defense through actin remodeling

Ruipu Wang[1,2], Dong Duan[3,*], Christian Metzger[2], Xin Zhu[2], Michael Riemann[2], Maria Pla[4] and Peter Nick[2]

[1]College of Agriculture, Guizhou University, Guiyang 550025, China
[2]Molecular Cell Biology, Botanical Institute, Karlsruhe Institute of Technology, Fritz-Haber-Weg 4, 76131 Karlsruhe, Germany
[3]Key Laboratory of Resource Biology and Biotechnology in Western China, Ministry of Education, College of Life Sciences, Northwest University, Xi'an 710069, China
[4]Institute for Food and Agricultural Technology (INTEA), University of Girona, Campus Montilivi (EPS-1), 17003 Girona, Spain
*Corresponding author. E-mail: dongduan@nwu.edu.cn

Abstract

In the current study, we used a grapevine cell line in which actin filaments are labeled by GFP to show that aluminum causes actin remodeling through activation of NADPH oxidase in the plasma membrane, followed by activation of phytoalexin synthesis genes. Elimination of actin filaments by latrunculin B disrupts gene activation and inhibition of MAPK signaling by the inhibitor PD98059. Interestingly, aluminum also induces the transcription of *ISOCHORISMATE SYNTHASE*, a key enzyme for the synthesis of salicylic acid, as well as *PR1*, a gene that is known to be responsive to salicylic acid. However, while salicylic acid responses are usually a hallmark of the hypersensitive response, aluminum-triggered defense is not accompanied by cell death. Both actin remodeling and gene activation in response to aluminum can be suppressed by the natural auxin indole acetic acid, suggesting that the actin response is not caused by nonspecific signaling. Further evidence for the specificity of the aluminum-triggered activation of phytoalexin synthesis genes comes from experiments in which plant peptide elicitors induce significant cellular mortality but do not evoke induction of these transcription. The response in grapevine cells can be recapitulated in grapevine leaf discs from two genotypes contrasting in stilbene inducibility. Here, aluminum can induce accumulation of the central grapevine phytoalexin, the stilbene aglycone *trans*-resveratrol; this is preceded by a rapid induction of transcription for *RESVERATROL SYNTHASE* and the regulating transcription factor *MYB14*. The amplitude of this induction reflects the general stilbene inducibility of these genotypes, indicating that the aluminum effect is not caused by nonspecific toxicity but by activation of specific signaling pathways. The findings are discussed in relation to a model in which actin filaments activate a specific branch of defense signaling, acting in concert with calcium-dependent PAMP-triggered immunity. This pathway links the apoplastic oxidative burst through MAPK signaling with the activation of defense-related transcription.

Introduction

Although static with respect to their location, plants live in a dynamic environment, which means that stress adaptation is crucial for their survival [1]. A central aspect of stress resilience is immunity against pathogens. While plants lack the adaptable immunity found in mammals, they have evolved two tiers of innate immunity [2]. For the first tier, plants sense and respond to microbes, including nonpathogens, via conserved pathogen-, microbe- and damage-associated molecular patterns (PAMPs, MAMPs, or DAMPs, respectively). Binding of the eliciting molecule to specific pattern recognition receptors (PRRs) triggers a broad basal immune response [3] termed PAMP-triggered immunity (PTI). Since PAMPs are essential for pathogen survival, selective pressure by the host toward the loss of these dangerous molecules is buffered by selective pressure to maintain these molecules because they are essential. This balance of antagonistic selective pressures has favored the evolution of effectors that can inhibit PTI and restore pathogenicity. In response, plants have acquired specific receptors to recognize these effectors, leading to the activation of the second tier of the immune system, called effector-triggered immunity (ETI), which is often specific for a particular pathogen or even a certain strain of a pathogen [4].

The recognition of PAMPs by PRRs is known to trigger calcium influx, which is followed by activation of mitogen-activated protein kinase (MAPK) cascades, in parallel with apoplastic oxidative burst. Consequently, transcription factors that will stimulate the expression of defense genes are induced[5]. Some of these events are shared with ETI [4], but the relative timing seems to differ. For instance, while calcium influx precedes oxidative burst during flagellin-triggered PTI of grapevine cells, the temporal order of these two stress inputs is reversed after

Received: October 16, 2020; **Accepted:** September 2, 2021; **Published:** 20 January 2022
© The Author(s) 2022. Published by Oxford University Press on behalf of Nanjing Agricultural University. This is an Open Access article distributed under the terms of the Creative Commons Attribution License (https://creativecommons.org/licenses/by/4.0), which permits unrestricted reuse, distribution, and reproduction in any medium, provided the original work is properly cited.

Downloaded from https://academic.oup.com/hr/article/doi/10.1093/hr/uhab016/6510205 by guest on 30 July 2026

elicitation with harpin, a bacterial trigger of an ETI-like response culminating in programmed cell death [6].

The two levels of immunity also differ with respect to regulation by phytohormones. While salicylic acid (SA) seems to activate ETI as an effective strategy against biotrophic pathogens, jasmonic acid (JA) is involved in the basal defense against necrotrophic pathogens. The antagonistic role of the two phytohormones is reflected in the antagonistic relationship of PTI versus ETI [7]. In suspended cells from the North American grape species Vitis rupestris, JA accumulated in response to PTI triggered by flg22 but not in response to harpin, a trigger of ETI-like defense [8]. In grapevine, different stilbenoids form the core of the phytoalexin defense [9]. These compounds are derived from the phenylpropanoid pathway and accumulate in response to pathogen infection as well as abiotic stress, such as mechanical damage or ultraviolet radiation [10]. Previous work from our group demonstrated that stilbene synthesis-related genes could be induced by both flg22-triggered PTI and harpin-triggered ETI-like pattern [6], as well as by UV-C radiation [11]. Chemotypes that are able to activate stilbene biosynthesis efficiently are significantly less susceptible to *Plasmopara viticola*, the causative agent of downy mildew [11], and to grapevine trunk diseases that are progressively emerging as a result of global climate change [12]. As a consequence of their importance for grapevine defense, the stilbene synthase family has enormously expanded in *Vitis*, whereby the coding sequences are mostly retained, while the promoter sequences have diversified, reflecting functional diversity [13, 14]. *STS47* (often referred to as resveratrol synthase) and *STS27* (often referred to as stilbene synthase) have been identified as central in the defense context. Both can be detected by specific oligonucleotide primers and thus are useful for monitoring resistance.

As described above, early signaling and the regulation of PTI and ETI by phytohormones can overlap to a certain extent, leading to the question of whether there are early cellular events associated with the dichotomy of the two layers of immunity. Comparative studies, where the responses to flg22 (triggering PTI) and harpin (a bacterial elicitor triggering an ETI-like type of defense) were compared side by side in suspension cells from either grapevine [6] or tobacco BY-2 (ref. 15), suggest that rapid reorganization of actin filaments seems to qualify as an early marker for cell death-related immunity. During the harpin-triggered ETI-like response, the NADPH-dependent oxidase respiratory burst oxidase homologue (RboH) is activated and generates superoxide. How this primary signal is transduced into cell death and/or gene activation has remained elusive. A few hints exist, however: a role for superoxide and phospholipase D (PLD) in actin remodeling in response to harpin has been inferred from inhibitor studies [16]. Furthermore, pharmacological modulation of actin filaments is accompanied by elevated expression of defense genes [17]. Modulation of actin dynamics has been shown to alter SA synthesis and signaling [18]. Although these findings indicate that actin filaments participate in defense signaling, the functional context is far from clear. Is actin remodeling necessary and sufficient for the activation of phytoalexin genes? Is actin bundling inevitably linked with cell death, or is it possible to separate these events?

One strategy to address these questions would be to trigger actin remodeling in the absence of a pathogen-related signal and to test whether this would activate defense responses. Actin filaments respond to numerous intracellular and extracellular signals [19]. In particular, abiotic stress factors that induce oxidative bursts often induce actin bundling, and actin is also involved in tolerance to these factors. For instance, aluminum, as an abundant metal and therefore of agricultural impact, is able to cause oxidative burst [20] and can induce actin bundling in tobacco seedlings [21]. Moreover, tobacco mutants generated by activation tagging that are tolerant to aluminum show constitutive bundling of actin, even in the absence of aluminum as a stressor [21]. Therefore, in the current study, we used the approach of triggering actin bundling by Al^{3+}. We followed the actin responses in a grapevine cell line expressing the fluorescent actin marker *GFP-AtFABD2* (ref. 22), and we investigated the resulting defense responses in grapevine cells and plants.

We show that Al^{3+} causes actin reorganization and the activation of phytoalexin synthesis transcription dependent on RboH but does not induce programmed cell death. This response is silenced by auxin and is not deployed by plant peptide elicitors, although these can evoke defense-related mortality, reflecting the specificity of the response. This actin reorganization in response to Al^{3+} induces genes for the synthesis of SA and phytoalexins, supporting a model where actin participates in a pathway involved in basal immunity by connecting the input from oxidative burst with the activation of defense genes.

Results

Actin is bundled in response to Al^{3+} in grapevine cells

To address the role of actin in defense, we used aluminum as a tool to induce actin remodeling based on our previous work demonstrating aluminum-dependent actin bundling in tobacco [21]. We therefore tested whether this response can also be evoked in grapevine cells. In control cells, actin was organized as a meshwork of fine filaments (Fig. 1A). Between these filaments, a few punctate signals were seen as well, for instance, in the perinuclear region. These punctate structures presumably represent nucleation complexes [23]. When the cells were incubated with $AlCl_3$ (200 μM), the actin filaments had, after 2 h, reorganized into dense bundles, often aligned with the long axis of the cell and detached from the membrane (Fig. 1B). In addition, the punctate signals increased in abundance. To statistically validate this phenomenon, actin bundling was assessed using a

Downloaded from https://academic.oup.com/hr/article/doi/10.1093/hr/uhab016/6510205 by guest on 30 July 2026

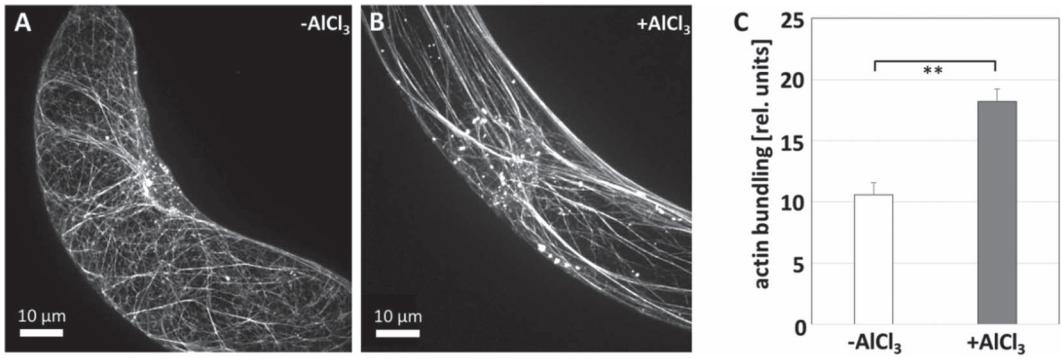

Figure 1. Response of actin filaments to aluminum ions. Representative images of grapevine cells expressing GFP fused to the actin marker fimbrin actin-binding domain 2 in the absence (A) or presence (B) of AlCl3 (200 μM, 2 h). (C) Quantification of the actin responses. Asterisks indicate significant differences with ** $P < 0.01$.

quantitative image analysis strategy (Fig. 1C). Compared to the control treatment, the aluminum treatment significantly increased the degree of bundling (by more than 60%).

To gain insight into the basis of the observed bundling, we used latrunculin B (LatB), a drug that irreversibly sequesters G-actin and prevents F-actin assembly such that actin polymerization is blocked. In response to 1 μM LatB (2 h), only short rods of actin were observed, accompanied by increased diffuse fluorescence in the cytoplasm and a higher incidence of punctate signals (Suppl. Fig. S1A). The fine filaments prevalent in control cells (Fig. 1A) were eliminated entirely, such that the quantification of actin bundling indicated a slightly increased value (compare white bars in Suppl. Fig. S1C with those in Fig. 1C). When LatB (1 μM) was administered in the presence of $AlCl_3$ (200 μM), the actin filaments were significantly longer (Suppl. Fig. S1B), and the degree of actin bundling was also slightly, but significantly ($P = 0.05$), increased compared to the situation without $AlCl_3$ (Suppl. Fig. S1C). Aluminum could rescue the effect of latrunculin B, albeit only partially. This would indicate that a part of the actin response to aluminum is attributable to a reduced turnover of actin filaments.

The response of actin to Al^{3+} requires the activity of NADPH oxidase

Reactive oxygen species (ROS), which are generated by the membrane-associated NADPH oxidase Reactive burst oxidase Homologue (RboH), represent an essential early signal for activating grapevine defense [6, 24]. Therefore, we asked whether the apoplastic oxidative burst generated by RboH- would be required for aluminum-dependent actin bundling (Fig. 2D). To investigate this possibility, we used diphenylene iodonium (DPI), a specific inhibitor of NADPH oxidases, to suppress the formation of apoplastic superoxide anions. When DPI was administered alone, it did not cause any significant bundling of actin (Fig. 2A, Fig. 2C). However, it was able to suppress the bundling response evoked by 200 μM Al^{3+} (Fig. 2B, Fig. 2C), demonstrating that the ROS generated by RboH are necessary for aluminum-induced actin bundling (Fig. 2D).

Genes related to the stilbene pathway are induced by Al^{3+} and are dependent on actin

A previous experiment indicated that RboH mediates the actin response to aluminum. From our previous work, we knew already that activation of RboH can induce the transcription of genes of the stilbene pathway [25]. Therefore, we asked whether actin is necessary for this activation. We targeted phenylammonium lyase (*PAL*) as the first committed step of the phenylpropanoid pathway and two subpopulations of the stilbene synthase family, resveratrol synthases (*STS47*) and canonical stilbene synthases (*STS27*), as markers for the potential activation of phytoalexin genes by Al^{3+}.

As shown in Fig. 3A, Al^{3+} (200 μM, 2 h) significantly induced the transcription of all three genes. The induction was slightly less pronounced for *STS27* (approximately 5-fold) than for *PAL* (approximately 6-fold) and *STS47* (approximately 7-fold). To test whether actin filaments are necessary for this activation (Fig. 3B), we first eliminated them by latrunculin B (Suppl. Fig. S1) before adding aluminum. For *STS47* and *STS27*, this pretreatment completely eliminated any induction by aluminum. An attenuation of activation was also observed for *PAL*, although a net induction of approximately 3-fold over the control remained. To test whether bundling actin was sufficient to induce phytoalexin expression, we probed the transcript levels of *PAL* in response to 1 μM phalloidin administered for 2 h in the absence of Al^{3+} (Suppl. Fig. S2). We observed a 10-fold induction, comparable to that seen for $AlCl_3$ treatment (Fig. 3A). Thus, bundling of actin filaments (achieved here by phalloidin) fully mimicked the effect of $AlCl_3$ on the induction of *PAL* (Fig. 3B).

Surprisingly, LatB administered in the absence of aluminum induced a conspicuous activation of all three genes as well (Fig. 3A), which for *PAL* and *STS47* even exceeded the response obtained by aluminum. In other words, two triggers that each induced gene expression when applied individually acted antagonistically if they

Downloaded from https://academic.oup.com/hr/article/doi/10.1093/hr/uhab016/6510205 by guest on 30 July 2026

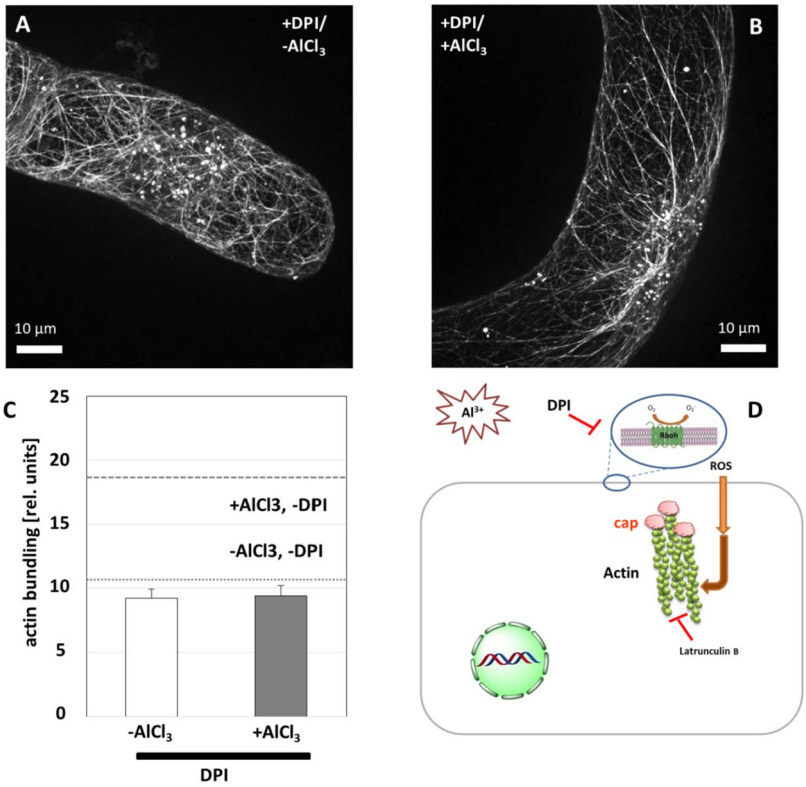

Figure 2. Effect of diphenylene iodonium (DPI) pretreatment (30 min, 20 μM) on the aluminum-induced response of actin filaments. Representative images of grapevine cells expressing GFP fused to the actin marker fimbrin actin-binding domain 2 in the absence (A) or presence (B) of AlCl3 (200 μM, 2 h) are shown. (C) Quantification of the actin response. The dashed line shows the amplitude of actin bundling in response to AlCl3 alone. The dotted line shows the value seen in the absence of DPI in untreated controls for comparison (see Fig. 1). (D) The working hypothesis was tested by this experiment.

were combined. This outcome was not only unexpected but even seemingly paradoxical.

To understand to what extent this induction of transcription was linked with PTI, which is initiated by calcium influx that can be measured as extracellular alkalinization, we probed for potential changes in extracellular pH in response to $AlCl_3$ (Suppl. Fig. S3). However, we did not observe any alkalinization; instead, the pH dropped slightly, due to the acidification caused by aluminum ions. Consistently, there was also no dependence on $GdCl_3$, an inhibitor of calcium channels that in PTI can block extracellular alkalinisation [6].

Transcription of *MYB14* are induced by Al^{3+} in an actin-dependent manner

The R2R3-MYB-type transcription factor *MYB14* has been shown to induce the transcription of the stilbene synthase promoter [26]. Therefore, in the current study, we tested whether *MYB14* transcription were induced by aluminum and, if so, whether this induction was dependent on actin in the same manner as *PAL*, *STS47*, and *STS27*. As shown in Fig. 4, Al^{3+} caused significant induction of *MYB14*, albeit to a lower amplitude (only approximately 2-fold) than *PAL*, *STS47* and *STS27* (Fig. 3A), which were induced between 5-fold (*STS27*) and 7-fold (*STS47*). This induction of *MYB14* by aluminum was suppressed by pretreatment with latrunculin B (Fig. 4). In contrast to *PAL*, *STS47*, and *STS27* (Fig. 3A), latrunculin B, if administered alone, did not induce *MYB14* expression. These results demonstrate that the activation of the transcription factor *MYB14* is dependent on actin.

Transcription of SA response and synthesis genes are induced by Al^{3+} in an actin-dependent manner

The experiments described above showed that aluminum induced defense-related transcription in an actin-dependent manner. Actin remodeling is often observed as a hallmark for ensuing programmed cell death. Since defense-related programmed cell death is usually deployed to encounter infection by biotrophic pathogens, a type of defense commonly regulated by salicylic acid (SA), we investigated the transcription of *PR-1* (pathogenesis related 1) [27] as a readout for SA-dependent gene expression. As shown in Fig. 5A, the steady-state transcript levels of *PR1* increased significantly in response to Al^{3+}, and this induction was decisively (by a factor of almost 3) suppressed by latrunculin B (Fig. 5A). The effect of aluminum could be efficiently mimicked by phalloidin (Suppl. Fig. S2), a compound that stabilizes filamentous actin (F-actin) by effectively suppressing actin dynamics. Latrunculin B alone yielded only a minor response (less than 25% of the response seen with Al^{3+}). While these data would place *PR1* downstream of actin, in a similar way as the

Downloaded from https://academic.oup.com/hr/article/doi/10.1093/hr/uhab016/6510205 by guest on 30 July 2026

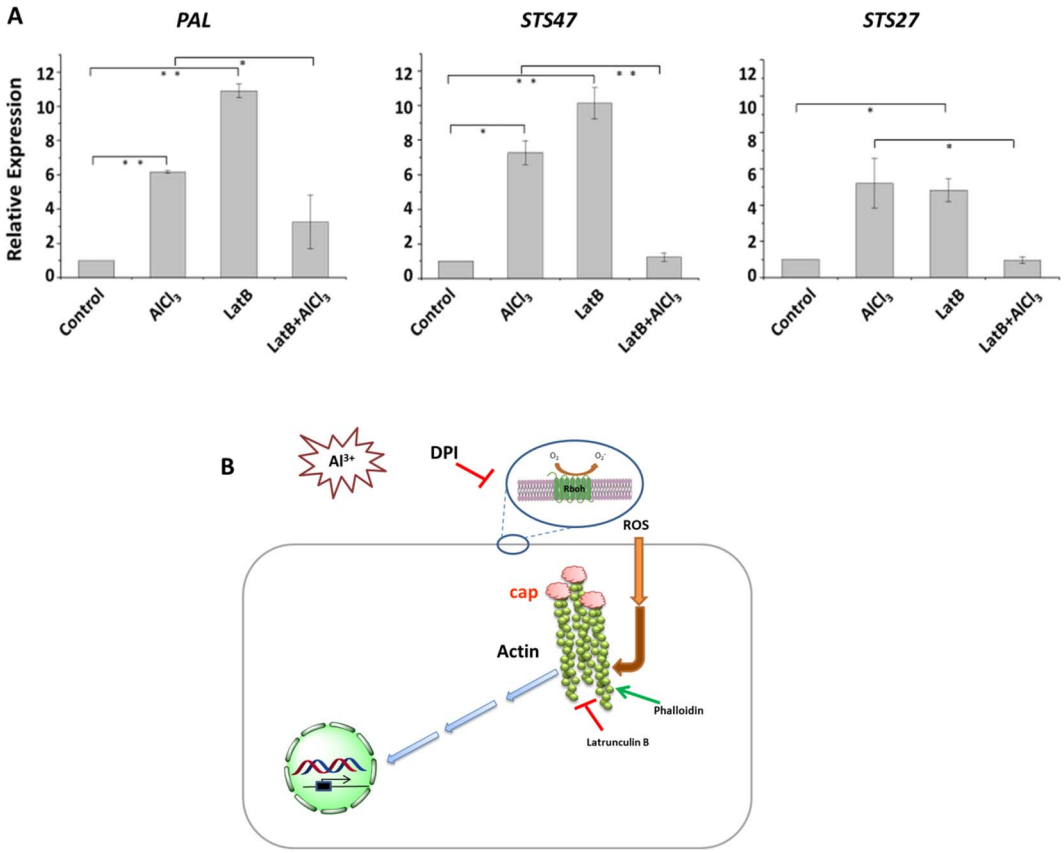

Figure 3. (A) Response of steady-state transcript levels of phenylammonium lyase (PAL), the resveratrol synthase subpopulation of the stilbene synthase family (STS47), and a canonical stilbene synthase (STS27) to 200 μM AlCl3 (2 h), 1 μM latrunculin B (LatB, 2 h), or a combination of latrunculin B (30 min) pretreatment followed by AlCl3 (2 h) treatment. Data represent the mean values and standard errors from three independent experimental series with three technical replicates for each biological replicate. Transcript levels were calibrated to EF-1α as an internal standard. Asterisks indicate significant differences (* $P < 0.05$ and ** $P < 0.01$). (B) The working hypothesis tested by this experiment.

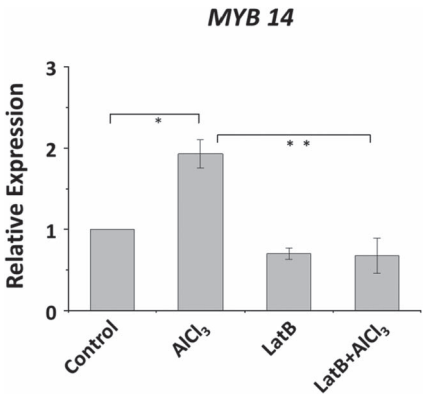

Figure 4. Response of steady-state transcript levels for MYB14 to either 200 μM AlCl3 (2 h), 1 μM latrunculin B (LatB, 2 h), or a combination of latrunculin B (LatB, 30 min) pretreatment followed by AlCl3 (2 h) treatment. Data represent the mean values and standard errors from three independent experimental series with three technical replicates for each biological replicate. Transcript levels were calibrated to EF-1α as an internal standard. Asterisks indicate significant differences (* $P < 0.05$ and ** $P < 0.01$).

phytoalexin synthesis genes (*PAL*, *STS47*, and *STS27*) and the transcriptional regulator *MYB14*, they also led to the following postulation:

If *PR1*, as an SA-responsive gene, is induce the transcription ofd by aluminum through actin-dependent signaling, there should also be a response of SA synthesis genes. Two biosynthetic pathways for SA are known [28] – one pathway uses cinnamonic acid as a substrate and therefore depends on the induction of *phenylalanine ammonium lyase* (*PAL*), while the other pathway uses isochorismate as a substrate and therefore depends on the induction of *isochorismate synthase* (*ICS*). The induction pattern for *PAL* had already been tested (Fig. 3A), but since this induction might also occur in the context of phytoalexin synthesis itself, it does not conclusively indicate a response to SA synthesis. Therefore, we analyzed the transcript levels of *ICS* and tested whether it followed the same activation pattern as the phytoalexin genes. As shown in Fig. 5B, Al^{3+} could induce *ICS* transcription significantly, although the induction was only approximately one-fifth of that seen for *PR1*. This aluminum response was completely suppressed by latrunculin B, and latrunculin B alone slightly induced *PR1* expression but rather significantly decreased *ICS* expression. In contrast to the pattern seen for *PR1* and *PAL*, phalloidin was not able to mimic aluminum with respect to the induction of *ICS* (Suppl. Fig. S2).

Downloaded from https://academic.oup.com/hr/article/doi/10.1093/hr/uhab016/6510205 by guest on 30 July 2026

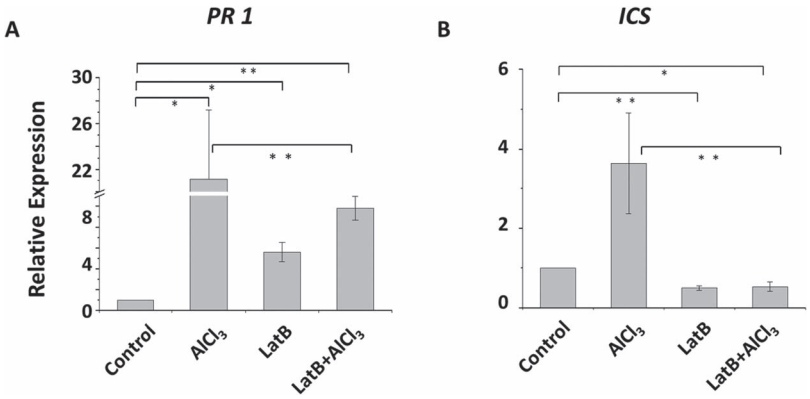

Figure 5. Response of steady-state transcript levels for pathogenesis-related 1 (PR1, A) and isochorismate synthase (ICS, B) to either 200 μM AlCl3 (2 h), 1 μM latrunculin B (LatB, 2 h), or a combination of Latrunculin B (LatB, 30 min) pretreatment followed by treatment with AlCl3 (2 h). The data represent the mean values and standard errors from three independent experimental series with three technical replicates for each biological replicate. Transcript levels were calibrated to EF-1α as an internal standard. Asterisks indicate significant differences (* $P < 0.05$ and ** $P < 0.01$).

Auxin can silence actin remodeling and gene expression in response to aluminum.

To probe the specificity of the response, we tried to interfere with actin using a natural signal, the plant auxin indole acetic acid (IAA), which can maintain actin in a debundled state [29]. In fact, in the presence of IAA, Al^{3+} did not induce any significant bundling (compare Fig. 6C and Fig. 1). Quantification (Fig. 6D) showed that bundling was reduced by a factor of 2 compared to the value found for aluminum without auxin. Neither the solvent control, a low concentration of DMSO (Fig. 6A), nor IAA alone (Fig. 6B) was able to produce any significant remodeling of actin filaments. Exogenous IAA not only suppressed actin remodeling despite the presence of aluminum but also almost entirely eliminated the induction of *PAL* and *STS47* transcription in response to Al^{3+} (Fig. 6E). This not only lends further support to the notion that actin remodeling is necessary for transcript induction but also shows that the actin response is integrated into signaling and thus is specific.

MAPK signaling is necessary for aluminum-triggered gene expression

A mitogen-activated protein kinase (MAPK) cascade is known to convey the defense signal from the plasma membrane to the nucleus, leading to changes in gene expression. This signal can be interrupted in grapevine cell cultures by the specific inhibitor PD98059, such that the activation of defense genes in response to elicitors is suppressed[6]. Therefore, we used the same approach to investigate whether MAPK signaling was involved in the activation of phytoalexin genes by Al^{3+}.

As shown in Fig. 7A, the MAPK inhibitor PD98059 fully suppressed the induction of *PAL*, *STS47*, and *STS27* transcription in response to aluminum. We then tested whether this inhibitor possibly interfered with aluminum-triggered actin remodeling. We used the same experimental design as in the gene expression experiments, i.e. the cells were treated for 30 min with PD98059, followed by an additional 2 hours with or without $AlCl_3$. We observed that the inhibitor by itself caused actin remodeling. In addition to mild bundling and the formation of longitudinal cables (Fig. 7B), punctate signals appeared in the perinuclear region. These perinuclear dots increased significantly in both size and number after Al^{3+} treatment (Fig. 7C). Although such dots had already been observed in response to aluminum alone (Fig. 1), their abundance and size differed to the extent that a different quantification strategy was required to incorporate these actin foci (Fig. 7D, E). We found a significant increase in the number of these foci after combined treatment with aluminum and PD98059 compared to PD98059 alone. While such foci were occasionally also seen in cells not treated with PD98059 (see Fig. 1B for example), their incidence was much lower in the absence of this inhibitor (Fig. 7E). These experiments are congruent with a model in which MAPK signaling acts downstream of aluminum-triggered actin remodeling (Fig. 7F). However, such changes to the actin foci were also observed in response to the inhibitor alone, indicating feedback from inhibited MAPK signaling (or the gene expression altered by this inhibited signaling), either to actin organization itself or to a step upstream of actin organization.

The effect of aluminum is specifically not linked with cytotoxicity

Since actin bundling often heralds programmed cell death [25], we wondered whether treatment with 200 μM Al^{3+} would increase mortality. We tested this hypothesis using the Evans blue dye exclusion assay; however, we failed to see any significant difference between Al^{3+}-treated cells and the mock control (Suppl. Fig. S4). Mortality was approximately 10% in both cases when scored 24 h after onset of the treatment. Thus, aluminum treatment triggered actin remodeling without inducing any programmed cell death.

To further clarify that the induction of defense genes in response to aluminum is not a nonspecific consequence of defense activation, we probed the effects of the plant

Downloaded from https://academic.oup.com/hr/article/doi/10.1093/hr/uhab016/6510205 by guest on 30 July 2026

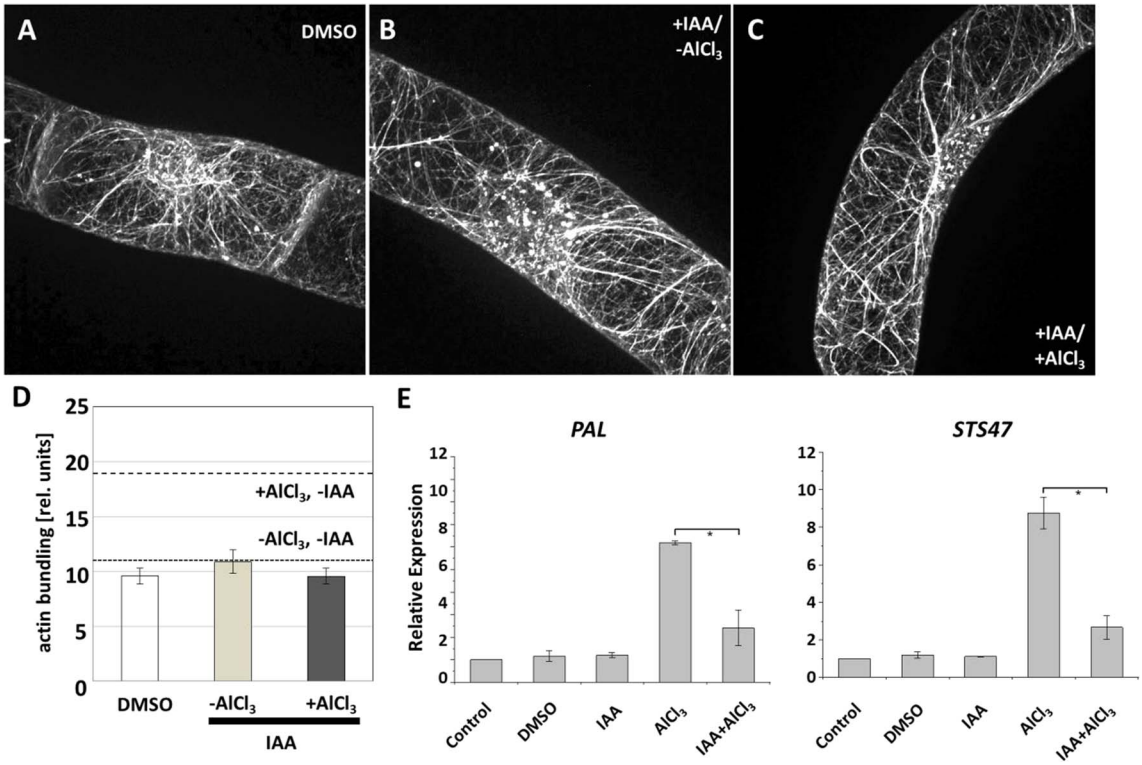

Figure 6. Effect of pretreatment with indole acetic acid (IAA) on the aluminum-induced response of actin filaments and defense-related transcription. Representative images of grapevine cells expressing GFP fused to the actin marker fimbrin actin-binding domain 2 in the absence (A) or presence (B) of IAA (10 μM, 2 h) and (C) after pretreatment with IAA for 30 min followed by treatment with AlCl3 for 2 h. (D) Quantification of the actin response. (E) Response of steady-state transcript levels for phenylammonium lyase (PAL) and the resveratrol synthase subpopulation of the stilbene synthase family (STS47) under the same conditions. Data represent mean values and standard errors from three independent experimental series with three technical replicates for each biological replicate. Transcript levels were calibrated to EF-1α as the internal standard. Asterisks indicate significant differences (* $P < 0.05$ and ** $P < 0.01$).

elicitor proteins (Pep). These peptides are encoded by the plants themselves, consist of more than twenty amino acids, and induce the transcription of defense-related programmed cell death [30, 31]. We treated cells with the two homologs from grapevine, VvPep1 and VvPep2, and observed that 1 μM of these peptides induced significant cell mortality within 24 h. However, this did not lead to any significant induction of the transcription of *PAL*, *STS47*, and *STS27* (Suppl. Fig. S5). Thus, the gene response is not a mere consequence of cellular damage but is induced by specific signaling pathways, such as those deployed by aluminum.

Differential activation of stilbene synthesis in different sylvestris chemovars

We wondered whether the pathway responsible for aluminum-induced activation of phytoalexin synthesis is active *in planta*. We selected two genotypes representing different chemovars: The V. vinifera variety 'Augster Weiss' was selected as representative low-stilbene chemovar, while the *V. sylvestris* genotype 'Hö29" was chosen as a high-stilbene chemovar. First, we tested whether induction by aluminum would reproduce the differences in transcript levels seen in the past for UV-C as a trigger. This was indeed the case (Fig. 8A): the transcription for both *MYB14* and *STS47* were induced more vigorously in Hö29 than in Augster Weiss. For *MYB14*, this difference appeared earlier (highly significant from 30 min after application of aluminum) compared to *STS47* (highly significant only at 60 min after application of aluminum). We next asked whether these differences in transcript levels would lead to a corresponding difference in the accumulation of the active stilbene *trans*-resveratrol. We measured the *trans*-resveratrol content by HPLC 24 h after treatment with aluminum and found that Hö29 accumulated more than twice as much *trans*-resveratrol as Augster Weiss (Fig. 8B). Since the induction of phytoalexin synthesis-related transcription by aluminum had been found to depend on the activation of RboH (Fig. 3), we wondered whether evidence of this oxidative burst could be detected in actual plant tissues. Since reactive oxygen species will react with membrane lipids, among other targets, an oxidative burst should lead to a transient increase in lipoxygenation, which can be detected by measuring the abundance of malondialdehyde (MDA). In fact, we were able to detect a rapid (from 15 min after the addition of aluminum) and transient (dissipating from 45 min after the addition of aluminum) increase in MDA levels by approximately 30% in Hö29, while no increase in MDA levels was observe in Augster Weiss (Fig. 8C). Thus, in the two chemovar representatives, aluminum triggered a differential response of MDA (indicative of oxidative burst), transcription of the stilbene regulator *MYB14*,

Downloaded from https://academic.oup.com/hr/article/doi/10.1093/hr/uhab016/6510205 by guest on 30 July 2026

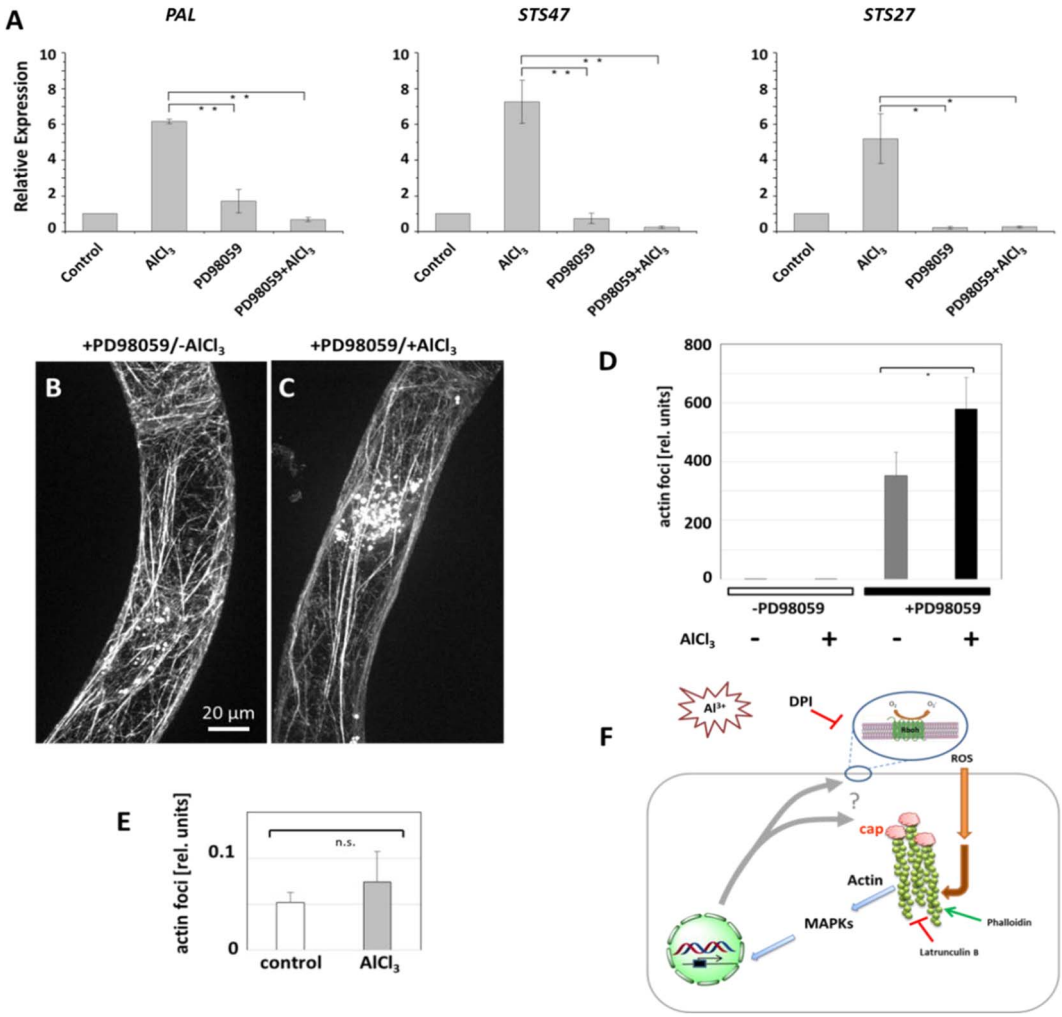

Figure 7. (A) Response of steady-state transcript levels of phenylammonium lyase (PAL), the resveratrol synthase subpopulation of the stilbene synthase family (STS47), and a canonical stilbene synthase (STS27) to either 200 μM AlCl3 (2 h), 50 μM PD98059 (2 h), or a combination of PD98059 (30 min) pretreatment followed by AlCl3 (2 h) treatment. Data represent mean values and standard errors from three independent experimental series with three technical replicates for each biological replicate. Transcript levels were calibrated to EF-1α as an internal standard. Asterisks indicate significant differences (* $P < 0.05$ and ** $P < 0.01$). (B) and (C) The responses of actin filaments to aluminum (200 μM, 2 h) in the presence of PD98059 (50 μM). Representative images of grapevine cells expressing GFP fused to the actin marker fimbrin actin-binding domain 2. (D) and (E) Quantification of the formation of actin foci. Because the response was much weaker in the absence of PD98059 in (D), values are replotted in (E) with a different scale. (F) The working hypothesis tested by this experiment.

the phytoalexin synthesis gene *STS47*, and eventually, accumulation of the active stilbene *trans*-resveratrol.

Discussion

In the current study, we provide evidence that remodeling actin filaments (in our experiments, induced by aluminum-dependent activation of the NADPH oxidase RboH) is sufficient to induce phytoalexin synthesis genes in grapevine. This activation of defense genes shares a dependence on MAPK signaling with flg22-triggered basal immunity but is independent of calcium influx. The remodeling of actin is shared with cell death-related defense responses. However, this aluminum-triggered defense response is not accompanied by cell death. Instead, aluminum also induces isochorismate synthase, a key enzyme for the synthesis of salicylic acid, as well as *PR1*, a gene known to be responsive to salicylic acid. In the following, we will discuss these findings in the context of a third defense pathway that bifurcates from cell death-related immunity (ETI) and merges with basal immunity (PTI); we will revisit the role of salicylic acid in basal immunity; we will suggest some conclusions on the nature and mechanisms of the actin remodeling that triggers this pathway; and we will provide an outlook on the potential applications for viticulture that can be derived from the current findings.

Actin-dependent and PTI signaling merge calcium influx and MAPK

The activation of calcium influx is a hallmark of PTI [32]. However, while aluminum can trigger an increase in phytoalexin synthesis transcription, it does not produce any extracellular alkalinization (Suppl. Fig. S3), indicating that this transcript induction is independent of calcium influx. On the other hand, in the presence of the

Downloaded from https://academic.oup.com/hr/article/doi/10.1093/hr/uhab016/6510205 by guest on 30 July 2026

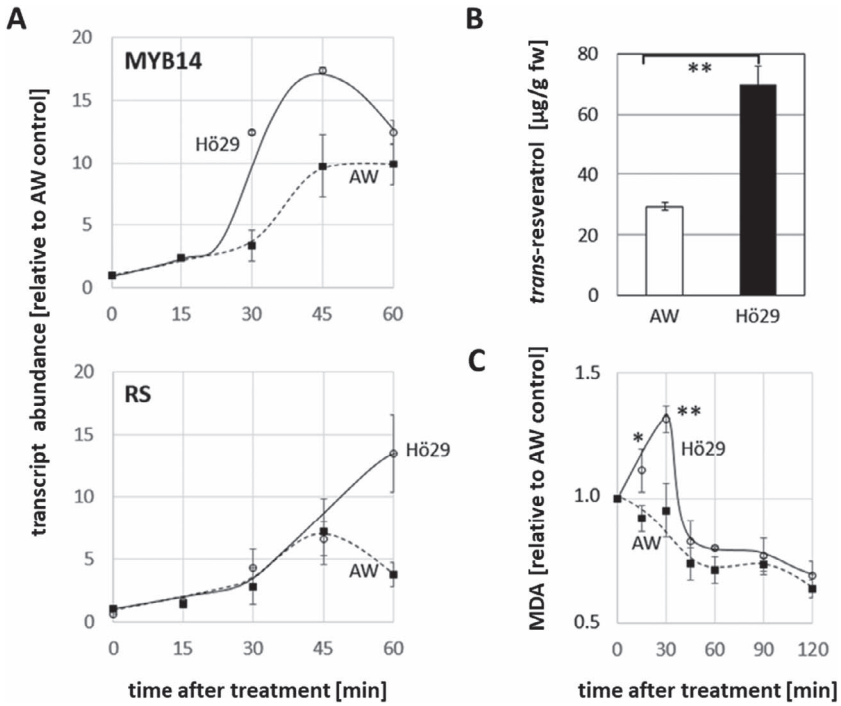

Figure 8. Responses of grapevine leaf discs to aluminum (1%) in the high-stilbene chemovar Vitis vinifera ssp. sylvestris genotype "Hö" 29 and the low-stilbene chemovar V. vinifera ssp. vinifera variety "Augster Weiss". (A) Time course of steady-state transcript levels of MYB14 and RS/STS47. (B) Contents of the active stilbene trans-resveratrol measured 24 h after treatment with aluminum. (C) The abundance of the lipid peroxidation product malondialdehyde (MDA) over time following treatment with aluminum. Data represent mean values and standard errors from three independent experimental series with three technical replicates for each biological replicate. Asterisks indicate significant differences (* $P < 0.05$ and ** $P < 0.01$).

specific MAPK inhibitor PD98059, the transcript response to aluminum was blocked completely (Fig. 7A). Thus, the most straightforward working model would place the joining of actin-dependent and PTI signaling downstream of calcium influx but upstream of MAPK activation. This model leads to two implications that are both supported by the literature. First, MAPK signaling should be activated by oxidative burst. In fact, this has been reported a lot [33], for instance, the serine–threonine kinase OXI1 could mediate the oxidative burst (ref. 34). Second, the MAPK cascade should be activated by modulation of actin dynamics. This implication has also been experimentally confirmed [35]. For instance, the activity of SIMK and SAMK, a MAP kinase from alfalfa, was activated when actin filaments were eliminated by latrunculin B [36, 37]; suppression of actin turnover by jasplakinolide also activated SIMK[36]. These authors also observed that a MEK1 inhibitor induced remodeling of plant actin, indicative of feedback of MAPK signaling to actin (consistent with our findings using PD98059, Fig. 7).

Defense-related actin remodeling can be separated from defense-related cell death

Actin remodeling has been recognized as an early event heralding subsequent programmed cell death [38–40]. In grapevine cells, the induction of programmed cell death by the bacterial elicitor harpin [16, 17], the stilbene aglycone resveratrol [25], or the oxylipin derivative 3-*cis*-hexenal [22] was preceded by actin remodeling involving depletion of the fine subcortical meshwork and massive bundling of transvascular actin cables. Thus, in these cases, actin remodeling was tightly correlated with programmed cell death. A correlation of these two events is a necessary condition for claiming a causal relationship between them. However, even though this correlation is tight, it cannot be considered sufficient to indicate causality.

In fact, actin remodeling of a similar type can be observed without any correlation with cell death. For instance, depletion of cortical actin and condensation of actin cables have also been observed in response to auxin depletion [41] or in response to activation of the plant photoreceptor phytochrome [42], both events that occur in the absence of any cell death.

The same conclusion was reached by our observation that aluminum did not cause any significant increase in mortality (Suppl. Fig. S4). Is actin remodeling just a side effect of these processes? However, this seems not to be the case either, because in the same cell system (*V. rupestris*), the induction of programmed cell death by harpin has been shown to be significantly mitigated by pretreatment with Latrunculin B [16], which provides evidence for actin being necessary to activate cell death.

Thus, while actin remodeling is usually accompanied by defense-related cell death, and suppression of actin remodeling impairs defense-related cell death, this apparently tight link is uncoupled in the case of aluminum treatment. The most straightforward explanation would be that actin remodeling has to coincide with a second signal to activate programmed cell death.

Downloaded from https://academic.oup.com/hr/article/doi/10.1093/hr/uhab016/6510205 by guest on 30 July 2026

This second signal cannot be the apoplastic oxidative burst generated by RboH because aluminum does trigger this response [43]. Moreover, we observed that actin remodeling in response to aluminum can be suppressed by diphenylene iodonium, which is indicative of RboH activity as a transducing event (Fig. 2). While in the case of an actual pathogen attack, apoplastic oxidative burst is accompanied by calcium influx, this does not seem to be the case for aluminum (Suppl. Fig. S3). Therefore, a parsimonious hypothesis would assume that calcium influx as a second signal is required to activate programmed cell death.

The actin-dependent response triggered by Al^{3+} is specific

Aluminum is a metal that frequently occurs in the soil but usually remains sequestered in complexes with different organic and inorganic anions. Upon acidification, for instance, through acid rain, it can leak out and cause considerable damage to roots [44]. This leads to the question of to what extent the phenomena described in the current work are specific and to what extent they might be nonspecific side effects of toxicity. There are several arguments for specificity, starting with the fact that the effects described here, both actin remodeling and the induction of transcription, are rapid responses, occurring within 2 hours, while we did not see any increase in mortality even after 24 hours (Suppl. Fig. S4). These observations are difficult to reconcile with a model in which actin remodeling and gene activation would be nonspecific consequences of proceeding cell death. The second argument is that aluminum-triggered actin remodeling and gene activation can be suppressed by specific inhibitors in the μM range. Latrunculin B is the most specific actin inhibitor known thus far; it sequesters actin monomers by binding at the interface between G-actin subunits, thus preventing them from assembly [45]. The concentration used here (1 μM) is only a factor of 5 greater than the K_d for latrunculin-actin binding. Diphenylene iodonium is a specific inhibitor of NADPH oxidase. Again, the concentration used here (10 μM) is close to the concentration of its target – a detailed discussion of its specificity can be found in a previous work [46]. The MAPK inhibitor PD98059 prevents the transfer of phosphate to the second tier of the cascade, such that MAPKK cannot be activated by the first MAPKKK [47] at concentrations between 50 and 100 μM, i.e. even higher than that used in the current study. The third argument for specificity of the actin response comes from an experiment here, where we found that the natural auxin indole acetic acid could suppress actin remodeling and activation of phytoalexin synthesis transcription (Fig. 6). This experiment shows that actin bundling is necessary for the induction of defense transcription and that suppressing this event by a physiological stimulus (the plant hormone auxin) will suppress the induction. Actin organization and auxin constitute a self-referring regulatory circuit in plants, whereby bundled actin filaments are not conducive to auxin transport, while additional auxin may activate its own transport by debundling actin [29]. This oscillator is antagonistically coupled to RboH-dependent actin remodeling and calibrates the balance between growth and defense [46]. This link between auxin, actin and RboH is also retained in grapevine cells [16], and our experiment recapitulates all physiological details of this highly specific phenomenon. As a fourth approach to probe this specificity, we asked whether defense evoking cell death might induce the same transcription that are induced by aluminum, as would be expected if this response were an nonspecific stress reaction. For this purpose, we used the grapevine homologs of plant elicitor peptides (Peps), which can activate defense pathways [48] and have also been used to increase the resistance of fruit crops against pathogens [49]. While VvPeps exerted a biological effect (inducing significant cell death), they failed to induce the transcription that were induced during the actin-dependent response to Al^{3+} (Suppl. Fig. S5). Thus, using four different lines of argument, the aluminum-triggered induction of defense transcription in an actin-dependent manner has been found to be specific and valid, supporting the specificity of this cellular response.

Calling for a role of salicylic acid signaling in basal immunity

The pathway activated by aluminum activates some features that, in grapevine cells, are usually associated with cell death-related immunity, such as actin remodeling or the activation of RboH [16]. On the other hand, aluminum does not induce cell death. We wondered, therefore, to what extent this would be reflected in activation of salicylic acid signaling, as salicylic acid is associated with defense against biotrophic pathogens, i.e. a condition in which cell death-related defense provides an evolutionary advantage, while PTI is associated with jasmonate signaling [50]. Additionally, for grapevine cells, jasmonate signaling seems to be exclusively linked to PTI [8]. Surprisingly, aluminum not only induced the transcription of phytoalexin genes but also induced the transcription of *isochorismate synthase*, encoding a key enzyme of salicylic acid biosynthesis (Fig. 5B), as well as the salicylic acid-responsive gene *PR1* (Fig. 5A). In both cases, the induction by aluminum could be inhibited by latrunculin B, providing evidence for the involvement of the actin-dependent pathway. A link between actin and salicylic acid signaling is apparently not confined to grapevine: In tobacco leaves, the levels of the marker genes *PR1* and *PR2* were significantly increased by treatment with cytochalasins [27]. A similar effect could be observed in Arabidopsis seedlings treated both with the actin polymerization inhibitors latrunculin B and depolymerization agent cytochalasin E. Here, the expression of *PR1*, *PR2* and *WRKY38* was increased after 6 h [18], mimicking the patterns seen for salicylic acid.

The coexistence of salicylic acid signaling with a defense pattern not accompanied by programmed cell death indicates that salicylic acid can be recruited for

Downloaded from https://academic.oup.com/hr/article/doi/10.1093/hr/uhab016/6510205 by guest on 30 July 2026

basal immunity, contradicting the current prevailing model. Additionally, this conclusion is in line with previous observations showing that salicylic acid can activate a specific stilbene synthase promoter allele from a wild Chinese grapevine species, *V. pseudoreticulata* [51].

What is the relationship between aluminum-triggered signaling and basal defense?

The fact that SA signaling can be activated by aluminum and acts in the context of basal immunity raises a new question: Is it possible to define the event at which the actin-dependent pathway merges with the signaling deployed in the context of PTI? The operational criterion for an event located downstream of this merging point would be that inhibition of this event would block both gene expression induced by flg22 and gene expression induced by aluminum. It seems that MAPK signaling meets this criterion because treatment of grapevine cells with the MAPK inhibitor PD98059 can entirely suppress the induction of all three tested genes involved in phytoalexin synthesis (i.e. *PAL*, *STS47*, and *STS27*, Fig. 7A), and the same was observed for the induction of *STS* by both flg22 and harpin [6]. This inhibitor acts at the MAPKK level of the cascade [52]. Specifically, for defense signaling, MKK1 has been suggested as a target [53]. Thus, at the second tier of MAPK signaling, flg22-triggered, harpin-triggered, and aluminum-triggered signal transduction seem to be confluent. Since aluminum, in contrast to flg22, fails to induce extracellular alkalinization (Suppl. Fig. S3), the merge point must be downstream of calcium influx. Furthermore, it must be located downstream of actin since latrunculin B can block the induction of gene expression by aluminum (Fig. 3A).

The fact that aluminum activates a key gene of SA synthesis (isochorismate synthase) and a marker gene for the SA response (PR1) does not mean that SA is part of the signaling responsible for the activation of phytoalexin synthesis genes. This is rather unlikely due to the time course. However, SA might act in a feedback loop that contributes to the persistence of defense activity. A straightforward mechanism would be the accumulation of intracellular ROS. The original idea that this might be caused by direct inhibition of catalase through salicylic acid [54, 55] has been discarded after decades of controversy and replaced by a model in which SA acts through a signaling network that regulates the expression and activities of enzymatic and nonenzymatic redox homeostasis [55]. The link with actin might come through phospholipase D: by binding to phospholipids, the substrates of phospholipid D, aluminum inhibits the formation of phosphatidic acids, as concluded from the fact that exogenous phosphatidic acids can mitigate the effect of aluminum in Arabidopsis seedlings [18].

There is a seemingly paradoxical observation, however: In our study, several of the genes that are induced by Al^{3+} are also significantly induced to the same extent by latrunculin B. The combination of Al^{3+} and latrunculin B eliminates this activation. Interestingly, the transcription factor MYB14 does not show this activation by latrunculin B. Although it appears paradoxical that two compounds that act antagonistically upon actin should exert the same effect on gene activation, this is not the first time this has been reported for phytoalexin synthesis genes in grapevine [17]. Additionally, for MAPK signaling, the activation of the MAP kinase SIMK by both latrunculin B and jasplakinolide reveals a similar paradox [36]. Activation of signaling by eliminating actin could be achieved by releasing an activator that had been tethered to actin, as has been proposed for the MAP kinases SIMK and SAMK [36, 37]. How signaling might be stimulated by suppression of actin turnover is more challenging to explain. One link might be Capping Protein, which can either be sequestered to the plasma membrane by phosphatidic acids, the products of the phospholipase D signaling hub, or block the elongation of actin filaments by blocking the barbed end [56]. Stabilization of actin might repartition Capping Protein from the membrane toward bundling actin cables, such that phosphatidic acid would be released for other signaling functions, such as activation of the Respiratory burst oxidase Homologue [46], leading to a self-amplifying signaling loop between actin and reactive oxygen species. The fact that some genes (*PAL*, *STS47*, *STS27*) show activation by both Al^{3+} and latrunculin B, while others (*MYB14*) are not induced by latrunculin B, indicates that the signaling pathways that initiate actin reorganization (one possibly through MAPK signaling and the other possibly through phosphatidic acid signaling) might be activated differentially and exert differing impacts on different target genes.

Outlook: From the cell culture to the vineyard – Routes toward application.

The induction of oxidative burst (Fig. 8C), transcription of MYB14 and *STS47* (Fig. 8A), and the accumulation of the bioactive phytoalexin *trans*-resveratrol (Fig. 8B) by Al^{3+} in leaf discs of grapevine indicate that the signaling chain discussed above is active not only in cell suspension but also *in planta*. Even genotype-dependent differences in the response amplitude between the more responsive *sylvestris* genotype Hö29 and the less responsive *vinifera* genotype Augster Weiss seen in earlier studies [11, 24] are preserved. The differences seen at the level of phytoalexin synthesis transcription (*STS47*) or the specific transcription factor triggering these genes (*MYB14*) are preceded by corresponding differences in the abundance of MDA. This indicates that the differential response of the two genotypes, which is also seen for UVC or the oomycete pathogen *Plasmopara viticola* [11], originates far upstream, possibly at the level of the abundance or activation of RboH. Aluminum-based compounds such as fosetyl aluminum (aluminum ethyl phosphite, AEP) have been used for decades to fight diseases caused by oomycetes, such as *Phytophthora* and *Plasmopara viticola*, but the mechanism is not well understood [57]. In addition, aluminum-based fungicides have

Downloaded from https://academic.oup.com/hr/article/doi/10.1093/hr/uhab016/6510205 by guest on 30 July 2026

been found to be effective in grapevine trunk diseases such as Esca syndrome [58] and exert a direct effect on the zoospores of *Plasmopara viticola* by interfering with the actin-dependent function of the contractile vacuole such that the zoospores burst [59]. However, the use of aluminum is problematic due to its negative ecological footprint [60]. Since aluminum induces defense through the activation of RboH, alternative approaches to stimulate RboH with a nontoxic compound would open the possibility to prime host immunity prior to its encountering a pathogen. Especially for P. viticola, the causative agent of downy mildew in grapevine, this would open new avenues for plant protection. Rather than relying on targeting the precise time window when the infecting zoospore still has not entered the stoma (leading to the excessive fungicide load characteristic of viticulture), this would enable a prophylactic treatment in which the host, rather than the pathogen, is addressed. In fact, we recently showed that RboH-dependent actin modeling and activation of defense genes can be evoked by treatment with glycyrrhizin, the active component of *Gan Cao* (*Glycyrrhiza uralensis*), a plant drug used in traditional Chinese medicine [61].

Materials and methods

Cell strains and plant material

Suspension cultures of V. rupestris [62] and a transgenic cell line of V. vinifera' Chardonnay', expressing the fluorescent actin marker *GFP-AtFABD2* [22], were cultivated in liquid medium containing 4.3 $g{\cdot}L^{-1}$ Murashige and Skoog salts (Duchefa, Haarlem, The Netherlands), 30 $g{\cdot}L^{-1}$ sucrose, 200 $mg{\cdot}L^{-1}$ KH_2PO_4, 100 $mg{\cdot}L^{-1}$ inositol, 1 $mg{\cdot}L^{-1}$ thiamine, and 0.2 $mg{\cdot}L^{-1}$ 2,4-dichlorophenoxyacetic acid (2,4-D), pH 5.8. The cells were subcultured weekly by inoculating 6 ml of stationary cells into 30 ml of fresh medium in 100 ml Erlenmeyer flasks and incubated at 27°C in the dark at 150 rpm on a horizontal shaker (KS250 basic, IKA Labortechnik, Staufen, Germany). For cultivation of the transgenic actin marker line, the medium was supplemented with kanamycin (50 $mg{\cdot}L^{-1}$). Since aluminum readily partitions into inactive complexes at neutral pH, especially in complex media, the complex MS medium was replaced by an acidified (pH 4.5) sucrose solution complemented with 3 mM $CaCl_2$ (ref. [63]). Experiments on plant elicitor proteins (Peps) did not require a change in the medium.

The Vitis vinifera ssp. sylvestris genotype "Hö29", and the V. vinifera ssp. *vinifera* variety "Augster Weiss" were cultivated and collected from the grapevine germplasm collection of the Botanical Garden of the Karlsruhe Institute of Technology.

Determination of cell mortality

To determine cell viability, cells treated with 200 μM $AlCl_3$, 1 μM VvPep1 and VvPep2 were stained at 24 h with Evans blue [64]. Cells were transferred into a custom-made staining chamber to remove the medium and then incubated with 2.5% Evans blue for 3–5 min. After washing three times with distilled water, cells were mounted on a slide and observed under a light microscope (Zeiss-Axioskop 2 FS, Differential Interference Contrast, 20× objective). Evans blue is membrane impermeable but can penetrate dead cells due to the breakdown of the plasma membrane, resulting in blue staining of the cell interior. Mortality was determined as the ratio of the number of dead cells to the total number of scored cells. For each time point, 1500 cells were scored in three independent experiments.

Stress treatments and inhibitor treatments

To impose UV-C stress, the leaf discs were irradiated for 2 min from a distance of 12.5 cm by a linear fluorescent bulb (λ_{max} = 254 nm, 15 W, Germicidal, General Electric, Japan). To induce aluminum stress, the cells were collected and resuspended in the medium described above (3% sucrose, 3 mM $CaCl_2$, pH 4.5) before adding $AlCl_3$ (Sigma, Deisenhofen) to a concentration of 200 μM[21]. For leaf discs, the treatment was conducted in petri dishes with $AlCl_3$ freshly dissolved in distilled water (1% w/v). To assess the role of actin filaments, Latrunculin B, an inhibitor of actin polymerization, and phalloidin, a compound stabilizing F-actin (both Sigma, Deisenhofen, Germany), were used at a final concentration of 1 μM diluted from an ethanolic stock solution. Diphenyleneiodonium chloride (DPI, Sigma–Aldrich, Deisenhofen, Germany), diluted to a final concentration of 20 μM from a stock solution in DMSO, was used to inhibit plasma membrane-based NADPH oxidase. Indole-3-acetic acid (IAA, Sigma–Aldrich, Deisenhofen, Germany), which could suppress actin bundling, was applied at a final concentration of 10 μM from a stock solution in DMSO. To examine the influence of MAPK signaling, the inhibitor PD98059 targeted to mitogen-activated protein kinase kinases (MAPKKs) (Sigma–Aldrich, Deisenhofen, Germany) was dissolved in DMSO and used at a final concentration of 50 μM. For further validation, VvPep1 and VvPep2 (plant elicitor peptide, INTEA, Spain) were administered at a final concentration of 1 μM. All treatments were accompanied by solvent controls, where the maximal concentration of solvent (never exceeding 0.1% v/v) used in the test samples was administered. If not stated otherwise, the treatments with aluminum or the inhibitors lasted for 2 hours. All experiments were performed at day 4 after subcultivation, when the culture had completed proliferation and was undergoing cell expansion. For the experiments with leaf discs, fresh, fully expanded leaves (plastochrones 4 and 5) of uniform size were used.

Visualization and quantification of actin responses in grapevine cells

The responses of actin filaments were followed in living grapevine cells of the actin marker line V. vinifera

Downloaded from https://academic.oup.com/hr/article/doi/10.1093/hr/uhab016/6510205 by guest on 30 July 2026

"Chardonnay" *GFP-AtFABD2* by spinning disc confocal microscopy on an AxioObserver Z1 (Zeiss, Jena, Germany) inverted microscope equipped with a laser dual spinning disc scan head from Yokogawa (Yokogawa CSU-X1 Spinning Disk Unit, Yokogawa Electric Corporation, Tokyo, Japan) and a cooled digital CCD camera (AxioCam MRm; Zeiss) [22]. To quantify the degree of actin aggregation, a modified strategy [65] was used. Intensity profiles were collected along a grid of equally spaced lines (four lines oriented perpendicular to the cell axis) using a line width of 10 pixels and the spline averaging option (ImageJ, https://imagej.nih.gov/ij/). The profile shows peaks and troughs corresponding to actin bundles and nonbundled actin (either G-actin or fine filaments that are not optically resolved). Aggregation of actin depletes this nonbundled actin such that the troughs are accentuated while the peaks become more prominent. This phenomenon can be quantified by calculating the standard error over the profile. This standard error can therefore be used as a readout of the degree of actin aggregation. Although this strategy is robust against variations in exposure parameters such as laser power, exposure time, or exposure gain, it was ensured that all images were recorded under the same magnification and exposure time by inactivating the automatic image acquisition routine of the software (ZEN, Zeiss, Jena). Approximately 3–5 cells per data point were used for quantification.

To estimate the reorganization of actin into foci (a phenomenon that was observed after treatment with the MAPK inhibitor PD98059), a different strategy was needed: The mean coverage of actin foci was estimated using the "analyze particles" tool of ImageJ. Images were first changed into 8-bit BW format and then transformed into a binary image using the thresholding tool. The value for the threshold was adjusted such that the dots (that were much brighter) remained while the filaments (that were dimmer) disappeared. To ensure that no residual filaments were selected for quantification, the circularity of the particle selection tool was set to 0.9–1 (i.e. only circular or ovoid structures were selected, while filamentous structures were excluded). To avoid picking up noise signals, the threshold for size selection was set to a minimum of 10 square pixels. Then, the readout "area" [in square pixels] was activated in the "set measurement" tool. After application of the "analyze particles" tool to the binary image, the results were exported into an Excel spreadsheet, and the total area of actin organized in foci was determined. Here, 20–25 cells per data point were used for quantification.

Analysis of extracellular pH

Extracellular alkalinization can be used as a rapid readout for the activation of plant immunity because it reports the coimport of the proton with calcium as an earliest known event of signaling. [66] Here, extracellular alkalinization was measured [17] after pre-equilibrating the cells on an orbital shaker for approximately 60 min before adding 200 μM $AlCl_3$, either with or without 20 μM $GdCl_3$, compared to a control without added compounds and a further control with 20 μM $GdCl_3$ alone.

Analysis of gene expression

The cells were collected, shock-frozen in liquid nitrogen and ground with a mortar and pestle (both heat-sterilized and then precooled) before extracting total RNA using a Universal RNA Purification Kit (Roboklon, Germany). In the case of leaf material, total RNA was isolated using the SpectrumTM Plant Total RNA Kit (Sigma, Deisenhofen, Germany), following the protocol of the manufacturer. Gene expression was analyzed at different time points after incubation with 200 μM $AlCl_3$. The extracted RNA was treated with DNA-free DNase (Roboklon, Germany) to remove potential contaminating genomic DNA. The mRNA was transcribed into cDNA using the M-MuLV cDNA Synthesis Kit (New England BioLabs; Frankfurt am Main, Germany) according to the instructions of the manufacturer.

Steady-state transcript levels of the selected genes (*PAL*, *STS47*, *STS27*, *MYB14*, *PR1* and *ICS*) were measured by quantitative real-time PCR (qRT-PCR)[11] using the oligonucleotide primers and PCR conditions given in Supplemental Table S1. To compare the transcript levels between different samples, the C_t values from each sample were normalized to the value for the *EF-1α* internal standard obtained from the same sample. These normalized C_t values were averaged over each technical triplicate. The difference between the C_t values of the target gene X and those for the *EF-1α* reference R were calculated as follows: $\Delta C_t(X) = C_t(X) - C_t(R)$. The final result was expressed as $2^{-\Delta\Delta Ct(X)}$. Each experiment was conducted in three biological replicates, i.e. independent experimental series.

Measurement of lipid peroxidation

Lipid peroxidation as a readout for oxidative damage was determined by measuring the reaction product malondialdehyde (MDA) according to standard protocols [67, 68] with some minor adjustment for grapevine leaves: the leaves (100 mg) were shock-frozen and ground in liquid nitrogen, the powder was vortexed for 45 seconds in 1 ml of 0.1 M phosphate buffer (pH 7.4) in a 2.0-ml Eppendorf tube and centrifuged for 4 minutes at 8000 g, and then the sediment was discarded. Subsequently, 200 μL of supernatant was added to a reaction mixture containing 750 μL acetic acid (20% w/v), 750 μL 2-thiobarbituric acid (aqueous solution, 0.8% w/v), 200 μL Milli-Q deionized water, and 100 μL sodium dodecyl sulfate (8.1% w/v). An identical reaction mixture in which the supernatant from the sample was replaced by an equal volume of buffer was used as a blank. The reaction mixture was incubated for 1 h at 98°C and then cooled to room temperature. The absorbance at 535 nm (specific signal) and 600 nm (background) was recorded by an ultraviolet spectrophotometer (Uvicon, Schott, Mainz). Lipid peroxidation was then calculated as μM MDA from A_{535} to A_{600} using an extinction coefficient of 155 mM^{-1} cm^{-1}.

Downloaded from https://academic.oup.com/hr/article/doi/10.1093/hr/uhab016/6510205 by guest on 30 July 2026

Acknowledgments

This work was supported by Interreg Upper Rhine (Vitifutur), co-financed by the European Union/European Regional Development Fund (ERDF), the German Federal Agency for Agriculture (Programme for Sustainable Agriculture, BÖLN), and by a fellowship from the China Scholarship Council to Dong Duan and Ruipu Wang. Hao Wang is acknowledged for kindly providing the FABD2-GFP actin marker line.

Data availability

The data that support the findings of this study are available in this article and the supplementary material. Other data not shown are available on request from the corresponding author.

Conflict of interest

We certify that the article is our original work. We declare that we have no conflicts of interest related to this work.

Supplementary data

Supplementary data is available at *Horticulture Research Journal* online.

References

1. Mittler R. Abiotic stress, the field environment and stress combination. *Trends Plant Sci*. 2006;**11**:15–9.
2. Jones JD, Dangl JL. The plant immune system. *Nature*. 2006;**444**:323–9.
3. Bigeard J, Colcombet J, Hirt H. Signaling mechanisms in pattern-triggered immunity (PTI). *Mol Plant*. 2015;**8**:521–39.
4. Tsuda K, Katagiri F. Comparing signaling mechanisms engaged in pattern-triggered and effector-triggered immunity. *Curr Opin Plant Biol*. 2010;**13**:459–65.
5. Withers J, Dong X. Post-translational regulation of plant immunity. *Curr Opin Plant Biol*. 2017;**38**:124–32.
6. Chang X, Nick P. Defence signalling triggered by Flg22 and Harpin is integrated into a different stilbene output in Vitis cells. *PLoS One*. 2012;**7**:e40446.
7. Ramirez-Prado JS, Abulfaraj AA, Rayapuram N *et al*. Plant immunity: from Signaling to epigenetic control of Defense. *Trends Plant Sci*. 2018;**23**:833–44.
8. Chang X, Seo M, Takebayashi Y *et al*. Jasmonates are induced by the PAMP flg22 but not the cell death-inducing elicitor Harpin in Vitis rupestris. *Protoplasma*. 2017;**254**:271–83.
9. Jeandet P, Douillet-Breul A-C, Bessis R *et al*. Phytoalexins from the Vitaceae: biosynthesis, phytoalexin gene expression in transgenic plants, antifungal activity, and metabolism. *J Agric Food Chem*. 2002;**50**:2731–41.
10. Langcake P, Pryce RJ. The production of resveratrol by Vitis vinifera and other members of the Vitaceae as a response to infection or injury. *Physiol Plant Pathol*. 1976;**9**:77–86.
11. Duan D, Halter D, Baltenweck R *et al*. Genetic diversity of stilbene metabolism in Vitis sylvestris. *J Exp Bot*. 2015;**66**:3243–57.
12. Khattab IM, Sahi VP, Baltenweck R *et al*. Ancestral chemotypes of cultivated grapevine with resistance to Botryosphaeriaceae-related dieback allocate metabolism towards bioactive stilbenes. *New Phytol*. 2021;**229**:1133–46.
13. Parage C, Tavares R, Rety S *et al*. Structural, functional, and evolutionary analysis of the unusually large stilbene synthase gene family in grapevine. *Plant Physiol*. 2012;**160**:1407–19.
14. Vannozzi A, Dry IB, Fasoli M *et al*. Genome-wide analysis of the grapevine stilbene synthase multigenic family: genomic organization and expression profiles upon biotic and abiotic stresses. *BMC Plant Biol*. 2012;**12**:130.
15. Guan X, Buchholz G, Nick P. The cytoskeleton is disrupted by the bacterial effector HrpZ, but not by the bacterial PAMP flg22, in tobacco BY-2 cells. *J Exp Bot*. 2013;**64**:1805–16.
16. Chang X, Riemann M, Liu Q *et al*. Actin as deathly switch? How auxin can suppress cell-death related defence. *PLoS One*. 2015;**10**:e0125498.
17. Qiao F, Chang XL, Nick P. The cytoskeleton enhances gene expression in the response to the Harpin elicitor in grapevine. *J Exp Bot*. 2010;**61**:4021–31.
18. Matouskova J, Janda M, Fiser R *et al*. Changes in actin dynamics are involved in salicylic acid signaling pathway. *Plant Sci*. 2014;**223**:36–44.
19. Wasteneys GO, Yang Z. New views on the plant cytoskeleton. *Plant Physiol*. 2004;**136**:3884–91.
20. Panda SK, Baluska F, Matsumoto H. Aluminum stress signaling in plants. *Plant Signal Behav*. 2009;**4**:592–7.
21. Ahad A, Nick P. Actin is bundled in activation-tagged tobacco mutants that tolerate aluminum. *Planta*. 2007;**225**:451–68.
22. Akaberi S, Wang H, Claudel P *et al*. Grapevine fatty acid hydroperoxide lyase generates actin-disrupting volatiles and promotes defence-related cell death. *J Exp Bot*. 2018;**69**:2883–96.
23. Maisch J, Fiserova J, Fischer L *et al*. Tobacco Arp3 is localized to actin-nucleating sites in vivo. *J Exp Bot*. 2009;**60**:603–14.
24. Duan D, Fischer S, Merz P *et al*. An ancestral allele of grapevine transcription factor MYB14 promotes plant defence. *J Exp Bot*. 2016;**67**:1795–804.
25. Chang X, Heene E, Qiao F *et al*. The phytoalexin resveratrol regulates the initiation of hypersensitive cell death in Vitis cell. *PLoS One*. 2011;**6**:e26405.
26. Höll J, Vannozzi A, Czemmel S *et al*. The R2R3-MYB transcription factors MYB14 and MYB15 regulate stilbene biosynthesis in Vitis vinifera. *Plant Cell*. 2013;**25**:4135–49.
27. Kobayashi Y, Kobayashi I. Depolymerization of the actin cytoskeleton induces defense responses in tobacco plants. *J Gen Plant Pathol*. 2007;**73**:360–4.
28. Chen Z, Zheng Z, Huang J *et al*. Biosynthesis of salicylic acid in plants. *Plant Signal Behav*. 2009;**4**:493–6.
29. Nick P. Probing the actin-auxin oscillator. *Plant Signal Behav*. 2010;**5**:94–8.
30. Blanvillain R, Young B, Cai Y-M *et al*. The Arabidopsis peptide kiss of death is an inducer of programmed cell death. *EMBO J*. 2011;**30**:1173–83.
31. Huffaker A, Pearce G, Ryan CA. An endogenous peptide signal in Arabidopsis activates components of the innate immune response. *Proc Natl Acad Sci U S A*. 2006;**103**:10098–103.
32. Gómez-Gómez L, Boller T. Flagellin perception: a paradigm for innate immunity. *Trends Plant Sci*. 2002;**7**:251–6.
33. Liu Y, He C. A review of redox signaling and the control of MAP kinase pathway in plants. *Redox Biol*. 2017;**11**:192–204.
34. Rentel MC, Lecourieux D, Ouaked F *et al*. OXI1 kinase is necessary for oxidative burst-mediated signalling in Arabidopsis. *Nature*. 2004;**427**:858–61.

Downloaded from https://academic.oup.com/hr/article/doi/10.1093/hr/uhab016/6510205 by guest on 30 July 2026

35. Samaj J, Baluska F, Hirt H. From signal to cell polarity: mitogen-activated protein kinases as sensors and effectors of cytoskeleton dynamicity. *J Exp Bot*. 2004;**55**:189–98.
36. Samaj J, Ovecka M, Hlavacka A *et al*. Involvement of the mitogen-activated protein kinase SIMK in regulation of root hair tip growth. *EMBO J*. 2002;**21**:3296–306.
37. Sangwan V, Orvar BL, Beyerly J *et al*. Opposite changes in membrane fluidity mimic cold and heat stress activation of distinct plant MAP kinase pathways. *Plant J*. 2002;**31**:629–38.
38. Gourlay CW, Ayscough KR. The actin cytoskeleton: a key regulator of apoptosis and ageing? *Nat Rev Mol Cell Biol*. 2005;**6**: 583–9.
39. Franklin-Tong VE, Gourlay CW. A role for actin in regulating apoptosis/programmed cell death: evidence spanning yeast, plants and animals. *Biochem J*. 2008;**413**:389–404.
40. Smertenko A, Franklin-Tong VE. Organisation and regulation of the cytoskeleton in plant programmed cell death. *Cell Death Differ*. 2011;**18**:1263–70.
41. Waller F, Riemann M, Nick P. A role for actin-driven secretion in auxin-induced growth. *Protoplasma*. 2002;**219**:0072–81.
42. Waller F, Nick P. Response of actin microfilaments during phytochrome-controlled growth of maize seedlings. *Protoplasma*. 1997;**200**:154–62.
43. Achary VM, Parinandi NL, Panda BB. Aluminum induces oxidative burst, cell wall NADH peroxidase activity, and DNA damage in root cells of Allium cepa L. *Environ Mol Mutagen*. 2012;**53**: 550–60.
44. Delhaize E, Ryan PR. Aluminum toxicity and tolerance in plants. *Plant Physiol*. 1995;**107**:315–21.
45. Coué M, Brenner SL, Spector I *et al*. Inhibition of actin polymerization by latrunculin a. *FEBS Lett*. 1987;**213**:316–8.
46. Eggenberger K, Sanyal P, Hundt S *et al*. Challenge integrity: the cell-penetrating peptide BP100 interferes with the Auxin-actin oscillator. *Plant Cell Physiol*. 2017;**58**:71–85.
47. Suri SS, Dhindsa RS. A heat-activated MAP kinase (HAMK) as a mediator of heat shock response in tobacco cells. *Plant Cell Environ*. 2008;**31**:218–26.
48. Albert M. Peptides as triggers of plant defence. *J Exp Bot*. 2013;**64**: 5269–79.
49. Ruiz C, Nadal A, Montesinos E *et al*. Novel Rosaceae plant elicitor peptides as sustainable tools to control Xanthomonas arboricola pv pruni in Prunus spp. *Mol Plant Pathol*. 2018;**19**:418–31.
50. Glazebrook J. Contrasting mechanisms of defense against biotrophic and necrotrophic pathogens. *Annu Rev Phytopathol*. 2005;**43**:205–27.
51. Jiao Y, Xu W, Duan D *et al*. A stilbene synthase allele from a Chinese wild grapevine confers resistance to powdery mildew by recruiting salicylic acid signalling for efficient defence. *J Exp Bot*. 2016;**67**:5841–56.
52. Cohen P. The search for physiological substrates of MAP and SAP kinases in mammalian cells. *Trends Cell Biol*. 1997;**7**:353–61.
53. Meszaros T, Helfer A, Hatzimasoura E *et al*. The Arabidopsis MAP kinase kinase MKK1 participates in defence responses to the bacterial elicitor flagellin. *Plant J*. 2006;**48**:485–98.
54. Chen Z, Silva H, Klessig DF. Active oxygen species in the induction of plant systemic acquired resistance by salicylic acid. *Science*. 1993;**262**:1883–6.
55. Klessig DF, Choi HW, Dempsey DA. Systemic acquired resistance and salicylic acid: past, present, and future. *Mol Plant-Microbe Interact*. 2018;**31**:871–88.
56. Li J, Blanchoin L, Staiger CJ. Signaling to actin stochastic dynamics. *Annu Rev Plant Biol*. 2015;**66**:415–40.
57. Dercks W, Buchenauer H. Comparative studies on the mode of action of aluminium ethyl phosphite in four Phytophthora species. *Crop Prot*. 1987;**6**:82–9.
58. Di Marco S, Osti F, Calzarno F *et al*. Effects of grapevine applications of fosetyl-aluminium formulations for downy mildew control on "esca" and associated fungi. *Phytopathol Mediterr*. 2011;**50**: 285–99.
59. Troster V, Setzer T, Hirth T *et al*. Probing the contractile vacuole as Achilles' heel of the biotrophic grapevine pathogen Plasmopara viticola. *Protoplasma*. 2017;**254**:1887–901.
60. Foy CD, Chaney RL, White MC. The physiology of metal toxicity in plants. *Annu Rev Physiol*. 1978;**29**:511–66.
61. Wang H, Riemann M, Liu Q *et al*. Glycyrrhizin, the active compound of the TCM drug Gan Cao stimulates actin remodelling and defence in grapevine. *Plant Sci*. 2021;**302**:110712.
62. Seibicke T, Rügner A, Neuhaus G *et al*. Assay system to screen for compounds inducing PR-gene expression in grape vine (Vitis spec.). *Induced Resistance in Plants against Insects and Diseases*. 2002;**25**:63–6.
63. Ikegawa S, Oohashi J, Murao N *et al*. A method for the determination of the hepatic enzyme activity catalyzing bile acid acyl glucuronide formation by high-performance liquid chromatography with pulsed amperometric detection. *Biomed Chromatogr*. 2000;**14**:144–50.
64. Gaff DF, Okong', -Ogola O O. The use of non-permeating pigments for testing the survival of cells. *J Exp Bot*. 1971; **22**:756–8.
65. Schwarzerova K, Zelenkova S, Nick P *et al*. Aluminum-induced rapid changes in the microtubular cytoskeleton of tobacco cell lines. *Plant Cell Physiol*. 2002;**43**:207–16.
66. Felix G, Regenass M, Boller T. Specific perception of subnanomolar concentrations of chitin fragments by tomato cells: induction of extracellular alkalinization, changes in protein phosphorylation, and establishment of a refractory state. *Plant J*. 1993;**4**: 307–16.
67. Heath RL, Packer L. Photoperoxidation in isolated chloroplasts. *Arch Biochem Biophys*. 1968;**125**:189–98.
68. Hodgson RA, Raison JK. Lipid peroxidation and superoxide dismutase activity in relation to photoinhibition induced by chilling in moderate light. *Planta*. 1991;**185**:215–9.

Downloaded from https://academic.oup.com/hr/article/doi/10.1093/hr/uhab016/6510205 by guest on 30 July 2026